Hindawi Publishing Corporation
Journal of Theoretical Chemistry
Volume 2013, Article ID 349870, 7 pages
http://dx.doi.org/10.1155/2013/349870

Research Article

Electron Momentum Density and Phase Transition in ZnS

N. Munjal,[1] M. C. Mishra,[2] G. Sharma,[3] and B. K. Sharma[2]

[1] *Department of Physics, Banasthali University, Banasthali 304022, India*
[2] *Department of Physics, University of Rajasthan, Jaipur 302004, India*
[3] *Department of Pure and Applied Physics, University of Kota, Kota 324010, India*

Correspondence should be addressed to G. Sharma; gsphysics@gmail.com

Received 10 March 2013; Accepted 10 June 2013

Academic Editors: H. Chermette, A. Kokalj, and T. Takayanagi

The electron momentum density distribution and phase transition in ZnS are reported in this paper. The calculations are performed on the basis of density functional theory (DFT) based on the linear combination of atomic orbitals (LCAO) method. To compare the theoretical Compton profile, the measurement on polycrystalline ZnS has been made using a Compton spectrometer employing 59.54 keV gamma rays. The spherically averaged theoretical Compton profile is in agreement with the measurement. On the basis of equal valence-electron-density Compton profiles, it is found that ZnS is less covalent as compared to ZnSe. The present study suggests zincblende (ZB) to rocksalt (RS) phase transition at 13.7 GPa. The calculated transition pressure is found in good agreement with the previous investigations.

1. Introduction

Zinc sulfide (ZnS) is an important member of the II–VI group due to its wide range of technological applications [1–4]. ZnS is a wide band gap (3.6 eV) material used in the optoelectronic devices such as optical memories and visual displays. It has two different crystal structures (zincblende and wurtzite), both of which exhibit direct band gaps. It is believed that ZnS transforms from the zincblende (ZB) or wurtzite (WZ) structure to the rocksalt (RS) structure and then to the β-Sn phase.

The electronic, optical, and structural properties of ZnS have been reported earlier by the number of research groups [5–36]. Liu and Chan [5] have performed density functional calculations within local density approximation (LDA) to explore the electronic properties of ZB ZnS with various impurities and defects. Khenata et al. [6] also have investigated the electronic properties of zinc monochalcogenides including ZnS using full-potential linear augmented plane-wave method plus local orbitals (FP-LAPW + lo) within LDA. Goswami et al. [7] have reported the electronic properties of low dimensional ZnS using density functional tight binding (DFTB) method in ZB and WZ modifications. Erbarut [8] have reported the electronic spectra of vacancies and their various charge states in cubic ZnS using Green's function approach within the localized orbital method. Benmakhlouf et al. [9] have predicted the pressure dependency on the electronic structure of ZnS using pseudopotential scheme. They observed that ZnS was found to exhibit direct and indirect band gaps under pressure. The band structure of ZnS has been investigated by Jaffe et al. [10] using an all-electron Hartree-Fock (HF) method including correlation corrections and evaluated the role of Zn 3d-band states in the electronic and optical properties of the material. The pressure dependence of the band gap in the ZB phase of ZnS has been investigated by Ves et al. [11] using linear-muffin-tin-orbital (LMTO) method within atomic-sphere-approximation (ASA). They found good agreement with the optical-absorption measurements. The structural properties of cubic ZnS have been investigated by Martins et al. [12] using plane wave pseudopotential (PW-PP) method and compared with an all electron LAPW method. Jaffe et al. [13] have reported ZB $\rightarrow$ RS transition in ZnS at 16.1 GPa using *ab initio* calculations based on HF-LCAO method. The phase transition and structural properties of ZnS in ZB, RS, β-Sn, and cinnabar (Cin) phases have been investigated by Nazzal and Qteish [14] using pseudopotential and local density approach. Qteish et al. [15] have investigated the phase transformation in ZnS under high pressure using first-principles

pseudopotential and full-potential linear muffin-tin orbital (FP-LMTO) methods. They found that there is no stable intermediate Cin phase of ZnS under pressure. Catti [16] has performed *ab initio* calculations to study the atomic pathway of the ZB to RS transition in ZnS using LCAO method within hybrid and LDA functionals. Using the tight-binding linear muffin-tin orbital (TB-LMTO) method, Gangadharan et al. [17] observed the ZB → RS phase transition at 15.5 GPa. Miao and Lambrecht [18] have reported the structural phase transition at 14.5 GPa in ZnS using the pseudopotentials and a plane-wave basis. The phase transition ZB → RS in ZnS has been investigated by Chen et al. [19] using the plane-wave pseudopotential (PW-PP) density functional theory. The structural phase transformation of ZnS under high pressure has also been investigated by Gupta et al. [20] using the first-principle PW-PP and FP-LAPW methods. *Ab initio* calculations of the electronic, linear, and nonlinear optical properties of zinc chalcogenides including ZnS and ZnSe have been investigated by Reshak and Auluck [21] using the full potential linear augmented plane wave (FP-LAPW) method. A number of studies are available in the literature on momentum densities of zincblende compounds, namely, AlAs, CdSe, BeS, BeSe, BeTe, GaSb, $Ga_{1-x}In_xN$, and BN [22–27].

Experimentally, pressure-induced phase transition in some II–VI compounds including ZnS has been investigated by Samara and Drickamer [28]. Piermarini and Block [29] have observed ZB → RS transition at 15.0 GPa using the ruby fluorescence line-shift based on the Decker equation of state (EOS). Pressure-induced structural changes in ZnS have been investigated by Zhou et al. [30] and Desgreniers et al. [31] using X-ray diffraction measurements. Using the energy dispersive X-ray diffraction technique, Pan et al. [32] have investigated the transition pressure of 11.5 GPa for the WZ → ZB and 16 GPa for the ZB → RS transitions.

Despite these studies, the ground state properties, that is, directional and spherically averaged Compton profiles of ZnS, have received little attention. It is well known that the Compton scattering is particularly sensitive to the momentum distribution of loosely bound electrons and therefore provides an interesting way to probe the electronic structure of materials [37, 38]. Measurements of line shape yield the Compton profile, $J(p_z)$, which is the one-dimensional projection of the electron momentum density along the scattering vector. Within impulse approximation,

$$J(p_z) = \iint_{-\infty}^{+\infty} n(\mathbf{p})\, dp_x dp_y, \tag{1}$$

where $n(\mathbf{p})$ is the electron momentum density and p_z is the electron momentum component parallel to the photon scattering vector [37–39]. Looking at the technological importance of zincblende ZnS and success of *ab-initio* methods has motivated us to explore the electron momentum density and structural phase transition in the compound.

2. Experimental Details

The ^{241}Am gamma-ray Compton spectrometer described by Sharma et al. [40] has been employed for the Compton profile measurement of ZnS. The sample having purity 99.99% was procured from Alfa Aesar, Johnson Matthey Co., USA. The ZnS sample of effective density 1.3606 gm/cm^3 was prepared from polycrystalline powder having thickness 3.2 mm. The sample was held vertical by affixing on the back of the lead covered brass slab with a hole of diameter 18.10 mm. The incident gamma rays of 59.54 keV from 5Ci annular ^{241}Am source were scattered at an angle $166^\circ \pm 3.0^\circ$ from the sample. The scattered radiation was analyzed using an HPGe detector (Canberra model, GL0110S) providing overall momentum resolution 0.6 a.u. The chamber was evacuated to about 1.33 Pa to reduce the contribution of air scattering. The spectra were recorded with a multichannel analyzer (MCA) with 4096 channels. The channel width was ~20 eV corresponding to 0.03 a.u. of momentum. The 2.75×10^4 counts were collected at the Compton peak, and the stability of the system was checked by using a weak ^{241}Am source.

The raw Compton data were corrected for several systematic corrections like background, instrumental resolution, absorption, cross section and multiple scattering, and so forth, using computer code of the Warwick group [41, 42]. We observed 4.7% contribution of multiple scattering in the momentum region −10 a.u. to +10 a.u. Finally, the corrected experimental data were normalized to 20.24 electrons in the range 0 to +7 a.u. being the area of free atom Compton profile [43]. In the present experimental setup, the K electrons of Zn contribute up to 2.2 a.u. only.

3. Theoretical Details

We employed first-principles LCAO method embodied in the CRYSTAL06 code [44] to explore the momentum density and phase transition in zincblende ZnS. In LCAO method each crystalline orbital $\psi_i(\mathbf{r}, \mathbf{k})$ is a linear combination of Bloch functions $\varphi_\mu(\mathbf{r}, \mathbf{k})$ defined in terms of local functions $\varphi_\mu(\mathbf{k})$, normally referred to as atomic orbitals. The local functions are expressed as linear combination of certain number of individually normalized Gaussian-type functions. For Zn and S, the local functions were constructed from the Gaussian type functions [45]. The Kohn-Sham Hamiltonian was constructed following the prescription of Dovesi et al. [44] while considering the exchange functional of Becke [46] and the Perdew-Burke-Ernzerhof (PBE) correlation functional [47, 48]. The self-consistent calculations were performed considering 145 $\vec{k}$ points in the irreducible Brillouin zone with tight tolerances. To achieve self-consistency 50 percent mixing of successive cycles was considered, and the self-consistency was achieved within 13 cycles.

4. Results and Discussion

In Table 1 we compare the experimental Compton profile for ZnS with the earlier measurement [33]. Also given here is the unconvoluted spherically averaged theoretical Compton profile computed from DFT-PBE scheme. The present measurement on ZnS is in good agreement with earlier data [33]. In order to compare the theoretical values with the present experiment, the theoretical values were convoluted with the

Table 1: The unconvoluted theoretical (DFT-PBE) and experiment Compton profiles of ZnS. All profiles are normalized at 20.24 electrons.

p_z (a.u.)	$J(p_z)$ in e/a.u.		
	DFT-PBE	Experiment	
		Present	Earlier [33]
0.00	10.271	9.729 ± 0.041	10.184 ± 0.05
0.10	10.231	9.691	10.112
0.20	10.066	9.554	9.922
0.30	9.701	9.310	9.622
0.40	9.441	8.973	9.224
0.50	8.936	8.573	8.746
0.60	8.416	8.130	8.209
0.70	7.802	7.648	7.637
0.80	7.159	7.141	7.059
1.00	5.981	6.186 ± 0.032	5.989 ± 0.04
1.20	5.111	5.410	5.162
1.40	4.714	4.793	4.608
1.60	4.311	4.333	4.238
1.80	3.953	3.922	3.927
2.00	3.610	3.599 ± 0.023	3.601 ± 0.035
3.00	2.201	2.245 ± 0.018	2.236 ± 0.020
4.00	1.380	1.422 ± 0.014	1.426
5.00	0.908	0.947 ± 0.011	0.953 ± 0.015
6.00	0.639	0.671 ± 0.009	0.668
7.00	0.469	0.495 ± 0.008	0.494

Gaussian function and normalized to 20.24 electrons from 0 to +7 a.u. To examine the agreement between theory and experiment, we plot in Figure 1 the difference profile deduced from the convoluted theoretical profile and the experiment. From Figure 1, it reveals that the electron momentum density based on the DFT-PBE calculations mostly overestimates the measurement in the momentum range $0.0 < p_z < 2.5$ a.u. Thereafter the trend is reversed. The maximum difference shown by the DFT-PBE with experimental $J(0)$ is about 3.7%. It is also seen that the differences are small in the high momentum region. It is expected because this is the region of core electrons which are unaffected in solid formation. From Figure 1, it can be inferred that DFT-PBE values are in overall good agreement with the experiment, but there are some residual differences especially in the low momentum region. This may possibly be due to the direct involvement of d-band electrons of Zn in determination of ground state properties of ZnS. The larger disagreement in the low momentum region also indicates that Lam and Platzman (LP) correction [49] may be useful in bringing the theory closer to the experiment below the Fermi momentum. Further, more accurate d-band basis sets may probably be helpful to estimate the momentum density accurately.

To examine the directional features theoretically, we consider the directional Compton profiles of ZnS along [100], [110], and [111] directions. We present the anisotropies derived from unconvoluted theory (DFT-PBE) in Figure 2. From Figure 2, it is visible that the anisotropies [100]–[110] and

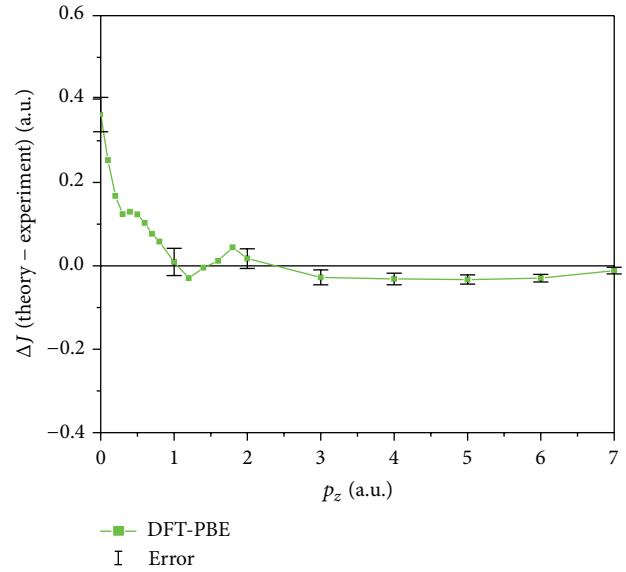

Figure 1: Difference between convoluted theoretical (DFT-PBE) and the experimental Compton profile of ZnS. Experimental errors ($\pm\sigma$) are also shown at a few points. The theoretical profile is convoluted with the Gaussian of 0.6 a.u. FWHM.

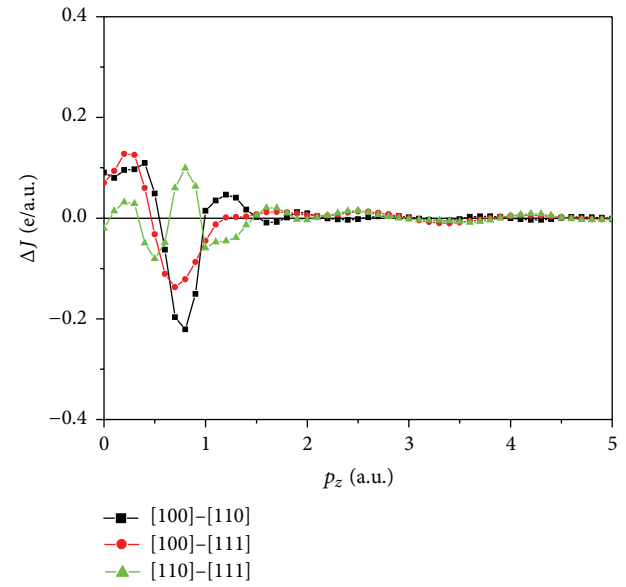

Figure 2: Compton profile anisotropies for ZnS. Anisotropies are computed following the DFT-PBE scheme. All anisotropies are obtained from unconvoluted directional Compton profiles.

[100]–[111] are positive in nature at $p_z = 0.0$ a.u. The maximum anisotropy is seen between [100] and [110] directions at $p_z = 0.8$ a.u. The figure also depicts that anisotropies are not observable in the high momentum region. The isotropic contribution due to core electrons dominates in determining the electron momentum density in this region and therefore anisotropies diminish. Measurements on single crystalline samples would be helpful to examine the directional features of bonding through anisotropies.

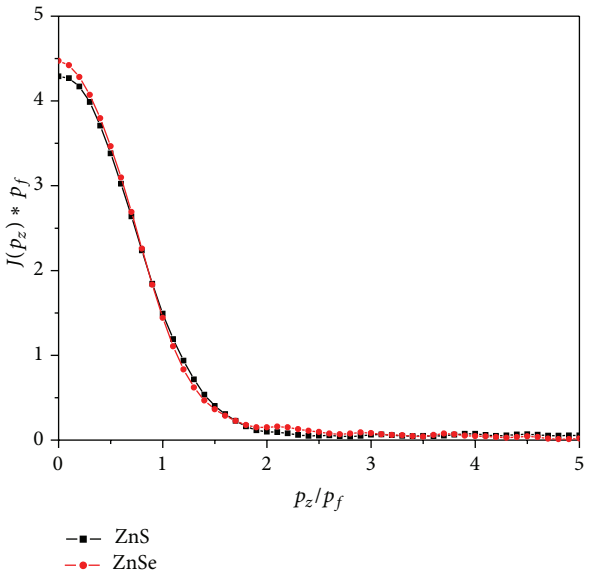

FIGURE 3: The EVED profiles of ZnS and ZnSe (p_F = 0.958 and 0.917 a.u. resp.). The EVED profiles are derived from experimental valence (experiment-convoluted core) Compton profiles, and both profiles are normalized to 4.0 electrons.

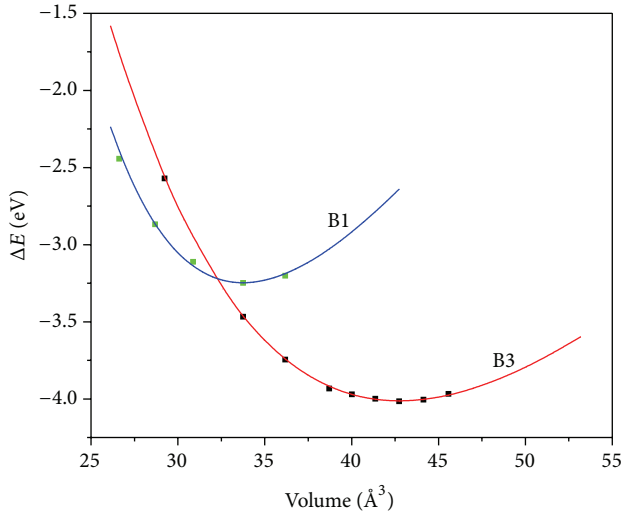

FIGURE 4: First-principles energy volume curves for B3 and B1 structures of ZnS calculated using DFT-PBE scheme. The scattered points show calculated energies and the solid lines show the fitted $E(V)$ curves according to Birch-Murnaghan equation of state (EOS).

To compare the nature of bonding in isovalent and isostructural zincblende ZnS and ZnSe, we have generated experimental equal valence electron density (EVED) profiles. In Figure 3, we plot the experimental EVED profiles of the two compounds deduced from experimental valence (experiment-convoluted core). For ZnSe, data is taken from our own earlier measurement [50]. The EVED profiles were derived by normalizing valence electron profiles to 4.0 electrons and scaling the resulting profiles by the Fermi momentum (p_F). For ZnS and ZnSe, p_F turned out to

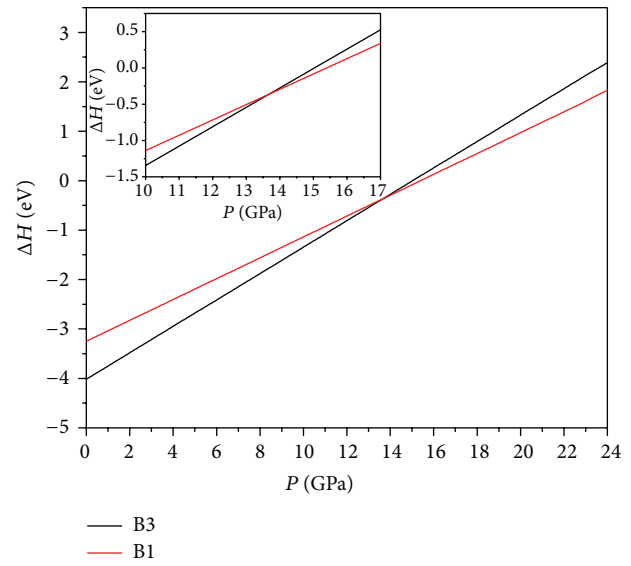

FIGURE 5: Enthalpy calculated from first-principles for B3 and B1 structures of ZnS using PBE correlation functional. At the transition pressure (P_t) 13.7 GPa curves cross each other.

be 0.958 and 0.917 a.u., respectively, using the expression $(3\pi^2 n)^{1/3}$, where n is the valence electron density. A number of researchers have shown that this scheme offers a way to understand the nature of bonding in solids [51–56]. Figure 3 depicts that the EVED profile corresponding to ZnSe is larger around the low momentum region compared to ZnS. As the larger value around low momentum is attributed to larger covalent character, it points out that ZnS is less covalent and hence more ionic than ZnSe. In contrast, J. C. Phillips [57] arrived at the opposite conclusion; that is, ZnSe shows larger ionic character as compared to ZnS.

To determine the structural parameters for the two structures, the total energy was calculated. Using the Birch Murnaghan equation of state (EOS) [58, 59], we obtained the energy-volume dependences $E = E(V)$. The total energy against volume curves for ZB (B3) and RS (B1) phases of ZnS is plotted in Figure 4. The energy states of B3 phase are below the B1 phase. It indicates the stability of the B3 phase. In Figure 4, the symbol represents our computed values and the curves represent fitting results to the following Birch-Murnaghan equation of state (EOS) [58, 59]:

$$E(V) = E_0 + \frac{9V_0B_0}{16}\left\{\left[\left(\frac{V_0}{V}\right)^{2/3} - 1\right]^3 B_0' + \left[\left(\frac{V_0}{V}\right)^{2/3} - 1\right]^2 \left[6 - 4\left(\frac{V_0}{V}\right)^{2/3}\right]\right\}, \quad (2)$$

where E_0 is the minimum energy, V_0 is the corresponding volume, and B_0 is the bulk modulus at zero pressure and $B_0' = dB_0/dP$. The lattice constant a_0, bulk modulus B_0, and its pressure derivative at zero pressure for both phases

Table 2: Calculated and experimental lattice parameter (a), bulk modulus (B_0), and its pressure derivatives (B_0') for ZnS in B3 and B1 phases.

	Present	Experimental	Other calculations
B3			
a (Å)	5.55	5.41 [34]	5.444 [20], 5.447 [20], 5.404 [19], 5.3998 [17], 5.58 [13], 5.39 [11]
B_0 (GPa)	70	76.9 [32], 89 [31], 75.0 [11]	73.21 [20], 71.61 [20], 71.22 [19], 80.97 [17], 92 [31], 75.9 [13], 82 [11]
B_0'	2.8	4.9 [32], 4 [11, 31]	3.78 [20], 3.79 [20], 4.705 [19], 2.3 [31] 4.7 [13], 4.2 [11]
P_t (GPa)	13.7	16.0 [32], 15.0 [29, 30], 14.7 [11], 15.4 [11]	15.2 [20], 17.2 [20], 15.4 [19], 17.5 [19], 14.5 [18], 15.5 [17], 14.7 [14], 14.5 [14], 16.1 [13], 19.5 [11], 19.9 [35], 20–23 [36]
B1			
a (Å)	5.13	5.06 [11]	5.1085 [20], 5.109 [20], 5.07 [19], 5.086 [17], 5.21 [13], 5.09 [11]
B_0 (GPa)	121.68	137.2 [24], 103.6 [11]	88.08 [20], 85.66 [20], 89.54 [19], 95.89 [17], 147 [31], 83.1 [13], 100.1 [11]
B_0'	4.101	4 [11, 24]	4.18 [20], 4.17 [20], 4.58 [19], 2.4 [31] 10 [13], 4.05 [11]

are calculated by fitting the above equation. These results are summarized in Table 2.

Now we discuss the structural transition B3 → B1 in ZnS. The transition pressure (P_t) is obtained from the enthalpy calculations. Here, we have considered zero temperature in our calculations. At this temperature the thermodynamically stable phase is that one with the lowest enthalpy, $H = E + PV$ at a given pressure. The calculated enthalpies of the two phases are plotted in Figure 5. The transition occurs when the enthalpy of the lower pressure phase coincides with some other phase at high pressure. After the point of intersection, the enthalpy of B1 becomes less than B3 phase. Hence, at low pressure the stable phase is B3 and at high pressure the stable phase is B1. The figure reveals structural transition from B3 to B1 at 13.7 GPa.

5. Conclusions

In this paper, electron momentum density distribution and phase transition in ZnS are reported. Compton profile measurement on polycrystalline ZnS supports the DFT-PBE calculation with the PBE correlation functional. The maximum anisotropy, that is, ~2.1% of $J_{iso}(0)$, is seen between [100] and [110] directions at $p_z = 0.8$ a.u. On the basis of EVED profiles, it is found that ZnS is less covalent compared to ZnSe. It has also been found that B3 is energetically favorable state, and B3 to B1 phase transition occurs at 13.7 GPa.

Acknowledgments

This work is financially supported by the CSIR through Project no. 03 (1205)/12/EMR-II. G. Sharma is also thankful to the Head of the Department of Pure & Applied Physics, University of Kota, for providing computational facilities.

References

[1] R. Rossetti, J. L. Ellison, J. M. Gibson, and L. E. Brus, "Size effects in the excited electronic states of small colloidal CdS crystallites," *The Journal of Chemical Physics*, vol. 80, no. 9, pp. 4464–4469, 1984.

[2] M. A. Haase, J. Qiu, J. M. DePuydt, and H. Cheng, "Blue-green laser diodes," *Applied Physics Letters*, vol. 59, no. 11, pp. 1272–1274, 1991.

[3] H. Kinto, M. Yagi, K. Tanigashira, T. Yamada, H. Uchiki, and S. Iida, "Photoluminescence studies of p- and n-type ZnS layers grown by vapor phase epitaxy," *Journal of Crystal Growth*, vol. 117, no. 1–4, pp. 348–352, 1992.

[4] G. D. Lee, M. H. Lee, and J. Ihm, "Role of d electrons in the zinc-blende semiconductors ZnS, ZnSe, and Z," *Physical Review B*, vol. 52, no. 3, pp. 1459–1462, 1995.

[5] H. J. Liu and C. T. Chan, "Density functional study on the electronic properties of ZnS:Te," *Physics Letters A*, vol. 352, no. 6, pp. 531–537, 2006.

[6] R. Khenata, A. Bouhemadou, M. Sahnoun, A. H. Reshak, H. Baltache, and M. Rabah, "Elastic, electronic and optical properties of ZnS, ZnSe and ZnTe under pressure," *Computational Materials Science*, vol. 38, no. 1, pp. 29–38, 2006.

[7] B. Goswami, S. Pal, and P. Sarkar, "A theoretical study on the electronic structure of ZnSe/ZnS and ZnS/ZnSe core/shell nanoparticles," *Journal of Physical Chemistry C*, vol. 112, no. 31, pp. 11630–11636, 2008.

[8] E. Erbarut, "The electronic spectra of vacancies in ZnS, ZnSe and ZnTe," *Solid State Communications*, vol. 128, no. 2-3, pp. 113–117, 2003.

[9] F. Benmakhlouf, A. Bechiri, and N. Bouarissa, "Zinc-blende ZnS under pressure: predicted electronic properties," *Solid-State Electronics*, vol. 47, no. 8, pp. 1335–1338, 2003.

[10] J. E. Jaffe, R. Pandey, and A. B. Kunz, "Correlated hartree-fock electronic structure of ZnO and ZnS," *Journal of Physics and Chemistry of Solids*, vol. 52, no. 6, pp. 755–760, 1991.

[11] S. Ves, U. Schwarz, N. E. Christensen, K. Syassen, and M. Cardona, "Cubic ZnS under pressure: optical-absorption edge, phase transition, and calculated equation of state," *Physical Review B*, vol. 42, no. 14, pp. 9113–9118, 1990.

[12] J. L. Martins, N. Troullier, and S. H. Wei, "Pseudopotential plane-wave calculations for ZnS," *Physical Review B*, vol. 43, no. 3, pp. 2213–2217, 1991.

[13] J. E. Jaffe, R. Pandey, and M. J. Seel, "Ab initio high-pressure structural and electronic properties of ZnS," *Physical Review B*, vol. 47, no. 11, pp. 6299–6303, 1993.

[14] A. Nazzal and A. Qteish, "Ab initio pseudopotential study of the structural phase transformations of ZnS under high pressure," *Physical Review B*, vol. 53, no. 13, pp. 8262–8266, 1996.

[15] A. Qteish, M. Abu-Jafar, and A. Nazzal, "The instability of the cinnabar phase of ZnS under high pressure," *Journal of Physics Condensed Matter*, vol. 10, no. 23, pp. 5069–5080, 1998.

[16] M. Catti, "First-principles study of the orthorhombic mechanism for the B3/B1 high-pressure phase transition of ZnS," *Physical Review B*, vol. 65, no. 22, Article ID 224115, 8 pages, 2002.

[17] R. Gangadharan, V. Jayalakshmi, J. Kalaiselvi, S. Mohan, R. Murugan, and B. Palanivel, "Electronic and structural properties of zinc chalcogenides ZnX (X = S, Se, Te)," *Journal of Alloys and Compounds*, vol. 359, no. 1-2, pp. 22–26, 2003.

[18] M. S. Miao and W. R. L. Lambrecht, "Universal transition state for high-pressure zinc blende to rocksalt phase transitions," *Physical Review Letters*, vol. 94, no. 22, Article ID 225501, 4 pages, 2005.

[19] X. R. Chen, X. F. Li, L. C. Cai, and J. Zhu, "Pressure induced phase transition in ZnS," *Solid State Communications*, vol. 139, no. 5, pp. 246–249, 2006.

[20] S. K. Gupta, S. Kumar, and S. Auluck, "Electronic and optical properties of high pressure stable phases of ZnS: comparison of FPLAPW and PW-PP results," *Optics Communications*, vol. 284, no. 1, pp. 20–26, 2011.

[21] A. H. Reshak and S. Auluck, "Ab initio calculations of the electronic, linear and nonlinear optical properties of zinc chalcogenides," *Physica B*, vol. 388, no. 1-2, pp. 34–42, 2007.

[22] N. Bouarissa, "High pressure dependence of positron states in zinc-blende boron nitride," *Materials Science and Engineering B*, vol. 94, no. 1, pp. 54–61, 2002.

[23] N. Bouarissa, "Positron behaviour in GaSb under pressure," *Journal of Physics and Chemistry of Solids*, vol. 61, no. 1, pp. 109–114, 2000.

[24] N. Bouarissa, "Composition dependence of positron states in zincblende $Ga_{1-x}In_xN$," *Philosophical Magazine B*, vol. 80, no. 10, pp. 1743–1756, 2000.

[25] M. S. Dhaka, G. Sharma, M. C. Mishra, K. B. Joshi, R. K. Kothari, and B. K. Sharma, "A study of electronic structure of CdSe by Compton scattering technique," *Physica B*, vol. 405, no. 17, pp. 3537–3542, 2010.

[26] N. Munjal, V. Sharma, G. Sharma, V. Vyas, B. K. Sharma, and J. E. Lowther, "Ab-initio study of the electronic and elastic properties of beryllium chalcogenides BeX (X = S, Se and Te)," *Physica Scripta*, vol. 84, no. 3, Article ID 035704, 2011.

[27] N. Munjal, G. Sharma, V. Vyas, K. B. Joshi, and B. K. Sharma, "Ab-initio study of structural and electronic properties of AlAs," *Philosophical Magazine*, vol. 92, no. 24, pp. 3101–3112, 2012.

[28] G. A. Samara and H. G. Drickamer, "Pressure induced phase transitions in some II–VI compounds," *Journal of Physics and Chemistry of Solids*, vol. 23, no. 5, pp. 457–461, 1962.

[29] G. J. Piermarini and S. Block, "Ultrahigh pressure diamond-anvil cell and several semiconductor phase transition pressures in relation to the fixed point pressure scale," *Review of Scientific Instruments*, vol. 46, no. 8, article 973, 7 pages, 1975.

[30] Y. Zhou, A. J. Campbell, and D. l. Heinz, "Equations of state and optical properties of the high pressure phase of zinc sulfide," *Journal of Physics and Chemistry of Solids*, vol. 52, no. 6, pp. 821–825, 1991.

[31] S. Desgreniers, L. Beaulieu, and I. Lepage, "Pressure-induced structural changes in ZnS," *Physical Review B*, vol. 61, no. 13, pp. 8726–8733, 2000.

[32] Y. Pan, S. Qu, S. Dong et al., "An investigation on the pressure-induced phase transition of nanocrystalline ZnS," *Journal of Physics Condensed Matter*, vol. 14, no. 44, pp. 10487–10490, 2002.

[33] B. K. Panda and H. C. Padhi, "Compton Scattering Studies in ZnS and ZnSe," *Physica Status Solidi (b)*, vol. 166, no. 2, pp. 519–523, 1991.

[34] O. Madelung, H. H. Landolt, and R. Börnstein, Eds., *Numerical Data and Functional Relationships in Science and Technology*, vol. 17, Springer, Berlin, Germany, 1982.

[35] J. R. Chelikowsky, "High-pressure phase transitions in diamond and zinc-blende semiconductors," *Physical Review B*, vol. 35, no. 3, pp. 1174–1180, 1987.

[36] T. Soma and H. M. Kagaya, "High-pressure NaCl-phase of tetrahedral compounds," *Solid State Communications*, vol. 50, no. 3, pp. 261–263, 1984.

[37] M. J. Cooper, "Compton scattering and electron momentum determination," *Reports on Progress in Physics*, vol. 48, no. 4, article 415, 1985.

[38] B. Williams, *Compton Scattering*, McGraw-Hill, New York, NY, USA, 1977.

[39] M. J. Cooper, P. E. Mijnarends, N. Shiotani, N. Sakai, and A. Bansil, *X-Ray Compton Scattering*, Oxford University Press, New York, NY, USA, 2004.

[40] B. K. Sharma, A. Gupta, H. Singh, S. Perkkiö, A. Kshirsagar, and D. G. Kanhere, "Compton profile of palladium," *Physical Review B*, vol. 37, no. 12, pp. 6821–6826, 1988.

[41] D. N. Timms, "Compton scattering studies of spin and momentum densities," *Unpublished Ph.D. thesis*, University of Warwick, Coventry, UK, 1989.

[42] J. Felsteiner, P. Pattison, and M. Cooper, "Effect of multiple scattering on experimental Compton profiles: a Monte Carlo calculation," *Philosophical Magazine*, vol. 30, no. 3, pp. 537–548, 1974.

[43] F. Biggs, L. B. Mendelsohn, and J. B. Mann, "Hartree Fock Compton profiles for the elements," *Atomic Data and Nuclear Data Tables*, vol. 16, no. 3, pp. 201–309, 1975.

[44] R. Dovesi, V. R. Saunders, C. Roetti et al., *CRYSTAL06 USer's Manual*, University of Torino, Turin, Italy, 2006.

[45] http://www.tcm.phy.cam.ac.uk/~mdt26/basis_sets/Zn_basis.txt, http://www.tcm.phy.cam.ac.uk/~mdt26/basis_sets/S_basis.txt.

[46] A. D. Becke, "Density-functional thermochemistry. III. The role of exact exchange," *Journal of Chemical Physics*, vol. 98, no. 7, article 5648, 5 pages, 1993.

[47] J. P. Perdew, K. Burke, and M. Ernzerhof, "Generalized gradient approximation made simple," *Physical Review Letters*, vol. 77, no. 18, pp. 3865–3868, 1996.

[48] J. P. Perdew, K. Burke, and M. Ernzerhof, "Generalized gradient approximation made simple [Phys. Rev. Lett. 77, 3865 (1996)]," *Physical Review Letters*, vol. 78, no. 7, article 1396, 1997.

[49] L. Lam and P. M. Platzman, "Momentum density and Compton profile of the inhomogeneous interacting electronic system. I. Formalism," *Physical Review B*, vol. 9, no. 12, pp. 5122–5127, 1974.

[50] V. Vyas, V. Purvia, Y. C. Sharma, K. B. Joshi, and B. K. Sharma, "Compton scattering study of ZnSe," *Physica Status Solidi (b)*, vol. 243, no. 6, pp. 1253–1262, 2006.

[51] W. A. Reed and P. Eisenberger, "Gamma-ray compton profiles of diamond, silicon, and germanium," *Physical Review B*, vol. 6, no. 12, pp. 4596–4604, 1972.

[52] M. C. Mishra, G. Sharma, R. K. Kothari, Y. K. Vijay, and B. K. Sharma, "Electronic structure of CaX (X = O, S, Se) compounds using Compton spectroscopy," *Computational Materials Science*, vol. 51, no. 1, pp. 340–346, 2012.

[53] G. Sharma, K. B. Joshi, M. C. Mishra et al., "Electronic structure of AlAs: a Compton profile study," *Journal of Alloys and Compounds*, vol. 485, no. 1-2, pp. 682–686, 2009.

[54] R. Kumar, N. Munjal, G. Sharma, V. Vyas, M. S. Dhaka, and B. K. Sharma, "Electron momentum density and phase transition in SrO," *Phase Transition*, vol. 85, no. 12, pp. 1098–1108, 2012.

[55] G. Sharma, P. Bhambhani, N. Munjal, V. Sharma, and B. K. Sharma, "Electronic properties of tin telluride: a first principles study," *Journal of Nano- and Electronic Physics*, vol. 3, no. 1, article 341, 2011.

[56] P. Bhambhani and G. Sharma, "*Ab-initio* study of phase transition and electron momentum density in PbTe," Accepted in Phase Transition, 2012.

[57] J. C. Phillips, "Ionicity of the chemical bond in crystals," *Reviews of Modern Physics*, vol. 42, no. 3, pp. 317–356, 1970.

[58] F. Birch, "Finite strain isotherm and velocities for single-crystal and polycrystalline NaCl at high pressures and 300°K," *Journal of Geophysical Research*, vol. 83, no. 3, pp. 1257–1268, 1978.

[59] J. P. Poirier, *Introduction to the Physics of the Earth's Interior*, Cambridge University Press, Cambridge, UK, 2000.